ACS OMEGA

Open Access

http://pubs.acs.org/journal/acsodf

Article

Graphene as a Sensor for Lung Cancer: Insights into Adsorption of VOCs Using vdW DFT

Viet Bac T. Phung,* Thi Nhan Tran, Quang Huy Tran, Thi Theu Luong, and Van An Dinh*

Cite This: *ACS Omega* 2024, 9, 2302−2313

Read Online

ACCESS | Metrics & More | Article Recommendations | Supporting Information

ABSTRACT: The adsorption mechanism of individual volatile organic compounds (VOCs) on the surface of graphene is investigated using nonempirical van der Waals (vdW) density functional theory. The VOCs chosen as adsorbates are ethanol, benzene, and toluene, which are found in the exhaled breath of lung cancer patients. The most energetically favorable configurations of the adsorbed systems, adsorption energy profiles, charge transfer, and work function are calculated. The fundamental insight into the interactions between the considered VOC molecules and graphene through molecular doping, i.e., charge transfer, is estimated. It is found that the adsorption energy is highly sensitive to the vdW functionals. Adsorption energies calculated by revPBE-vdW are in good agreement with the available experimental data, and the revPBE-vdW functional can cover well the physical phenomena behind the adsorption of these VOCs on graphene. Bader charge analysis shows that 0.064, 0.042, and 0.061e of charge were transferred from the graphene surface to ethanol, benzene, and toluene, respectively. All of the considered VOCs act as electron acceptors from graphene. By analyzing the electronic structure of the adsorption systems, we found that the energy level of the highest occupied molecular orbitals of these considered VOCs is shifted backward toward the Fermi level. The interaction of the VOCs with the π and π^* states of the C atoms in graphene breaks the symmetry of graphene, leading to the opening of a band gap at the Fermi level. The adsorption of these considered VOCs onto the pristine graphene produces a band gap of 5−12 meV.

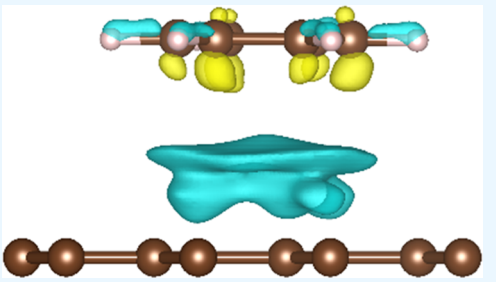

1. INTRODUCTION

Exhaled breath contains numerous volatile organic compounds (VOCs) of both exogenous and endogenous origin.[1] Endogenous VOCs are produced by biological processes, including oxidative stress and inflammation in the human body[2,3] as well as by invading microorganisms.[4] Once produced, these VOCs are excreted into the bloodstream and diffuse into the lungs, where they are exhaled. Oxidative stress and inflammation cause changes in the composition of the VOCs excreted by the affected organ and, subsequently, in exhaled breath. Additionally, microorganisms can produce specific compounds that lead to different VOC profiles in exhaled breath. Detection and monitoring of VOCs in human breath are useful for screening, diagnosing, and detecting various diseases, such as lung cancer, the intestinal tract, asthma, etc., at an early stage. Chemical breath analysis for VOCs was found to be feasible for the noninvasive diagnosis and follow-up of inflammatory processes in cystic fibrosis lung disease.[5] Detection of VOCs can allow for disease diagnosis before other physical symptoms appear, and early diagnosis can greatly improve the clinical outlook.[6] Unfortunately, currently available methods for early cancer diagnosis are scarce and inefficient. In fact, the concentration of VOCs in the breath of cancer patients is different from that of healthy individuals.[7] Exhaled breath contains over 200 VOCs, such as aromatic hydrocarbons, alicyclic hydrocarbons, and chain hydrocarbons. Therefore, VOCs in exhaled breath are being considered as possible biomarkers for various pulmonary diseases. However, accurate measurements of extremely low concentrations of VOCs in exhaled breath have been technically challenging, without being contaminated by atmospheric VOCs.[8] Therefore, the development of new sensors that can detect VOCs at low concentrations corresponding to the early stages of cancer is desirable.

Two-dimensional (2D) materials are promising for nanosensors that can detect volatile organic compounds (VOCs) at low concentrations thanks to their large surface area-to-volume ratio. In recent years, the development of variable gas sensing conductors based on various 2D nanomaterials has attracted great interest in the field of breath diagnostics.[9−15] These sensing devices are portable, compact, and inexpensive, with high accuracy for quick results. To be useful for breath analysis, these sensors require high sensitivity and good selectivity for various VOCs. This problem can be solved only by explicitly

Received: August 19, 2023
Revised: December 7, 2023
Accepted: December 13, 2023
Published: January 3, 2024

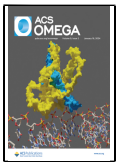

exploring the mechanism of gas adsorption, applying suitable gas-sensitive materials, and optimizing the sensor structures and operation.

Adsorption of gas molecules on graphene can be evaluated by quantum mechanical calculations based on density functional theory (DFT).[16,17] Karlický et al. studied the adsorption of some small organic molecules on graphene, such as acetone, ethanol, dichloromethane, benzene, and toluene, using both theoretical and experimental methods.[18,19] Experimental measurements of the adsorption energies of some organic molecules on graphene have also been performed with small errors.[20] However, due to limitations in experimental characterization, the adsorption behaviors of gas molecules on the surface of graphene have been widely investigated by first-principles calculations, which are meaningful for the application of graphene.[21] The strength of the interaction between graphene and the VOCs was estimated by DFT calculations, wave function theory, and empirical calculations. In order to quantify and identify the nature of the interaction of adsorbed molecules on graphene, it requires a high reliability of the results obtained from the DFT calculations. However, the results obtained with the local density approximation (LDA) and generalized gradient approximation (GGA) are often inadequately credible.[22,23] The reason is that the adsorption mechanism of a small organic molecule on the surface of 2D materials is mainly governed by the long-range electron correlation, i.e., the van der Waals (vdW) interaction.[24] Therefore, the vdW interaction plays a fundamental role in the adsorption of small organic molecules on graphene.[25] Including the vdW interactions in DFT calculations is very important to qualify and identify the adsorption properties and electronic responses of graphene to VOC gases. DFT calculations including vdW interactions have been routine practice to study the gas adsorption mechanism of graphene. Adsorption energies obtained from ab initio molecular dynamics (MD) employing the nonlocal optB86b-vdW functional were found to be in good agreement with the experimental data.[18,19,25]

Despite the availability of these studies, there is still a lack of sufficient theoretical comparative studies on the physics and chemistry of VOC molecule adsorption onto pristine graphene surfaces for healthcare applications, specifically in the design of sensors for the detection and monitoring of VOCs in human breath. Although the adsorption of toxic gases has been actively investigated, there is a lack of systematic investigation of the adsorption of VOCs on 2D materials. The challenge is to develop a calculation method to determine the most stable configurations and the diffusion possibilities of the VOCs on the 2D materials surface, as the structure of the VOC molecules is much more complex with many degrees of freedom, and it is not easy to scan all of the orienting possibilities of the VOCs on the surface. The determination of the adsorption structure is necessary to accurately estimate the parameters for evaluating the adsorption efficiency.

Understanding gas adsorption at finite temperatures is essential for accurately predicting and optimizing these processes. Finite-temperature effects, which are often overlooked in traditional studies that focus on absolute zero, can have a significant impact on the behavior of adsorbate molecules on various surfaces. In this context, there are several research papers exploring the influence of a finite temperature on gas adsorption. These studies examine how temperature variations affect the adsorption of VOCs on different surfaces and discuss key findings from recent research in this field. One notable study by Dai et al.[26] investigated the temperature dependence of adsorption and desorption dynamics of gas molecules on boron-doped graphene. This research delves into the temperature dependence of gas adsorption on boron-doped graphene, shedding light on the dynamic behavior of adsorbate molecules at various temperatures. The study provides a comprehensive analysis of the adsorption process and its temperature-related variations. Focusing on short alkanes adsorption, Göltl and Hafner[27] explored how temperature and dispersion forces influence adsorption in protonated chabazite by performing MD simulations. The study emphasized the role of temperature in shaping adsorption behavior, adding valuable insights into our understanding of finite-temperature effects. Kaneko et al.[28] investigated the effect of preheating temperature on single-gas molecule adsorption on graphene oxide; this study offers insights into the temperature-dependent behavior of gas molecules during adsorption and highlights the importance of considering temperature effects in practical applications.

Zero-point energy (ZPE) is the energy associated with the vibrational motion of atoms or molecules at absolute zero temperature. The degrees of freedom describe how molecules move and rotate in three-dimensional space. As the temperature increases, these degrees of freedom play a significant role in determining the overall energy and thermodynamic properties of the system. In DFT simulations for finite-temperature effects, the inclusion of this energy correction in the calculated total energy enables us to account for the effect of translational and rotational motion of molecules, even at absolute zero temperature. Although we recognized the importance of incorporating ZPE corrections when reporting reactions involving hydrogen-containing species,[29] the weak interaction between gas and graphene ensures that the kinetic energy remains relatively consistent, leading to only a minimal variation in adsorption energy. The inclusion of ZPE corrections would have a very slight effect on adsorption energies and does not alter the trends concerning the most stable adsorption sites.

In this study, we aim to investigate the adsorption mechanism of some VOCs onto the surface of pristine graphene and the response of the graphene due to gas adsorption using quantum simulation methods. Our research focuses on investigating the adsorption mechanism and electronic responses of graphene to VOC gases, with a specific aim of developing graphene-based sensors for detecting lung cancer. We assess graphene's gas-sensitive detection capabilities for VOCs, and we study the adsorption mechanisms at 0 K. Therefore, we evaluate the fundamental properties of VOCs adsorption on graphene using the DFT method at 0 K, without considering external influences. We have considered the particular patterns of the VOCs found in exhaled breath, such as ethanol, benzene, and toluene molecules. Since van der Waals (vdW) forces play a fundamental role in the structure of molecules and the behavior of physical adsorption systems, the adsorption energy profiles are calculated using different approximations of vdW interactions to study their effects in these systems. A comparative analysis of the structural and electronic properties of graphene adsorbed with ethanol, benzene, and toluene is also provided. Furthermore, this computational study can provide insights into the mechanism of VOC adsorption on graphene.

https://doi.org/10.1021/acsomega.3c06159
ACS Omega 2024, 9, 2302−2313

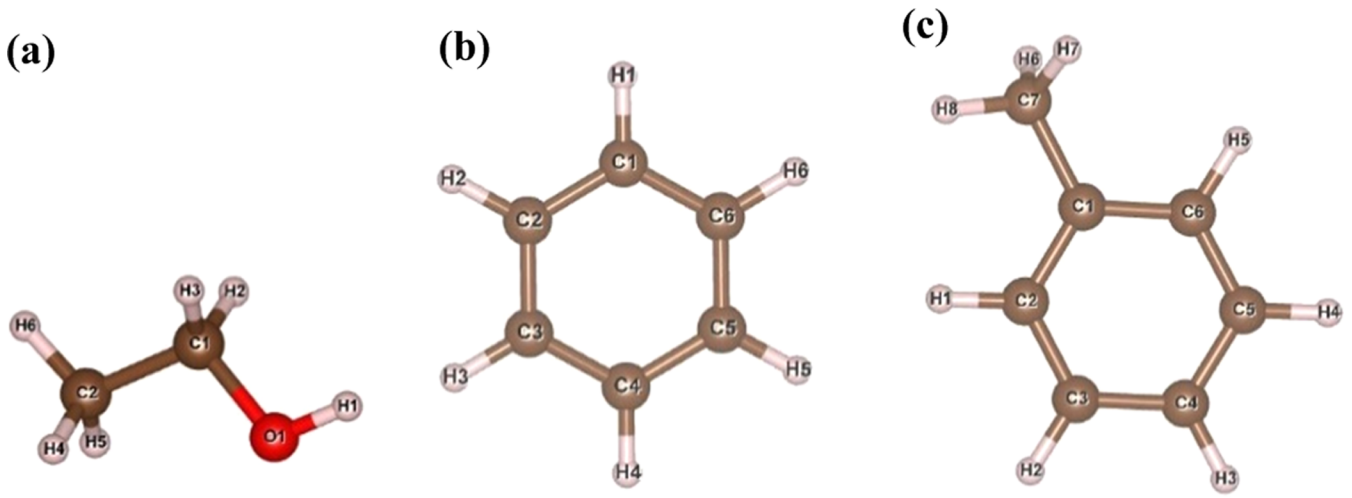

Figure 1. Molecular structures of ethanol (a), benzene (b), and toluene (c): the brown, white, pink, and red spheres represent C, H, and O atoms, respectively.

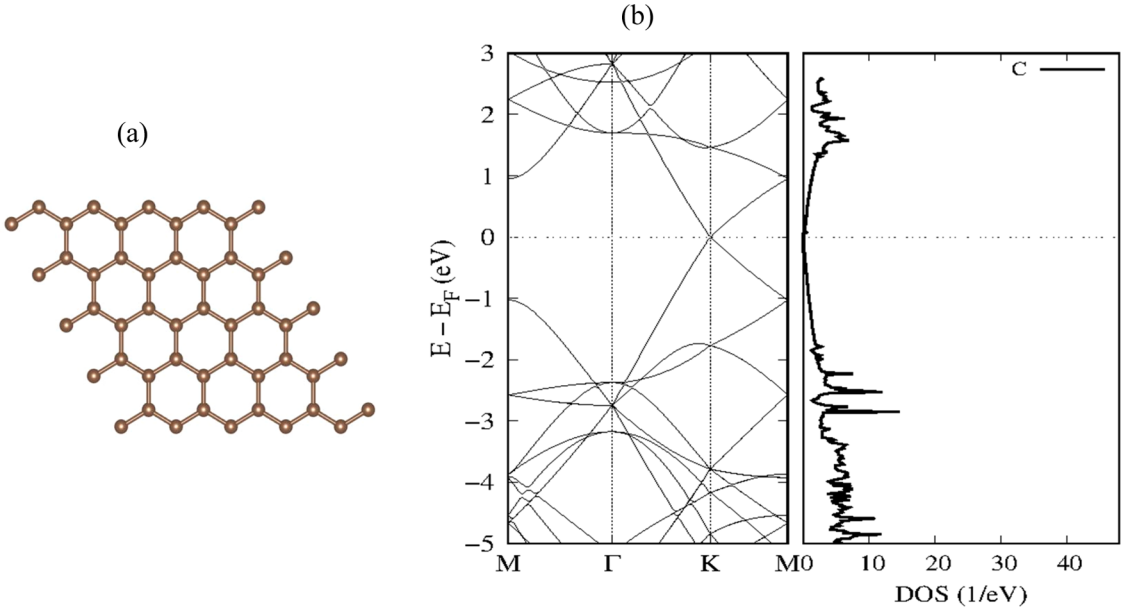

Figure 2. Optimized structure of pristine graphene (a) and band structure along the principal directions of the hexagonal Brillouin zone (along the *M*−Γ−*K*−*M* path) and the total DOS of the pristine graphene (b).

2. COMPUTATIONAL METHODOLOGY

The adsorption mechanisms of ethanol, benzene, and toluene molecules on the surface of a graphene 4 × 4 supercell were investigated through theoretical calculations within the framework of DFT.[9,10] Ab initio calculation simulations were performed using the density functional method implemented in the software *Vienna Ab initio Simulation Package* (VASP)[30] with the aid of high-performance computers. VASP uses density functional approaches for solving the Schrödinger equation of many-particle systems.

A graphene surface model containing 32 carbon atoms, built from the geometries obtained through experimental data, was put into a supercell with single-layered periodicity and a large vacuum space (25 Å) to eliminate the possible interaction between adjacent layers. A cutoff energy of 550 eV for the plane-wave basis set was utilized. Brillouin zone integration was performed on a γ-centered points scheme with 3 × 3 × 1 and 12 × 12 × 1 K-point mesh for the geometry optimization and electronic calculations, respectively. These parameters were carefully chosen after several calculations to obtain well-converged results. All of the structures were fully relaxed until the maximum Hellmann−Feynman force acting on each atom was less than 0.001 eV/Å.

The possibilities of orienting the VOCs on the surface of graphene are systematically investigated using the Computational DFT-based Nanoscope tool.[31] With this tool, the gas molecule is considered as the tip of a scanner, which moves on the adsorbent surface and rotates around its center of mass (COM) to find a stable adsorption configuration. The images of the potential energy surfaces (PES) for different positions of the adsorbates on graphene are explored to determine the most stable configurations and diffusion possibilities. Using this tool, the problem of handling the complex configurations of the VOCs and adsorbents can be solved.[32−34] The minimum energy configurations as well as the optimized distance from the VOC molecules to the adsorbent surface will be

https://doi.org/10.1021/acsomega.3c06159
ACS Omega 2024, 9, 2302−2313

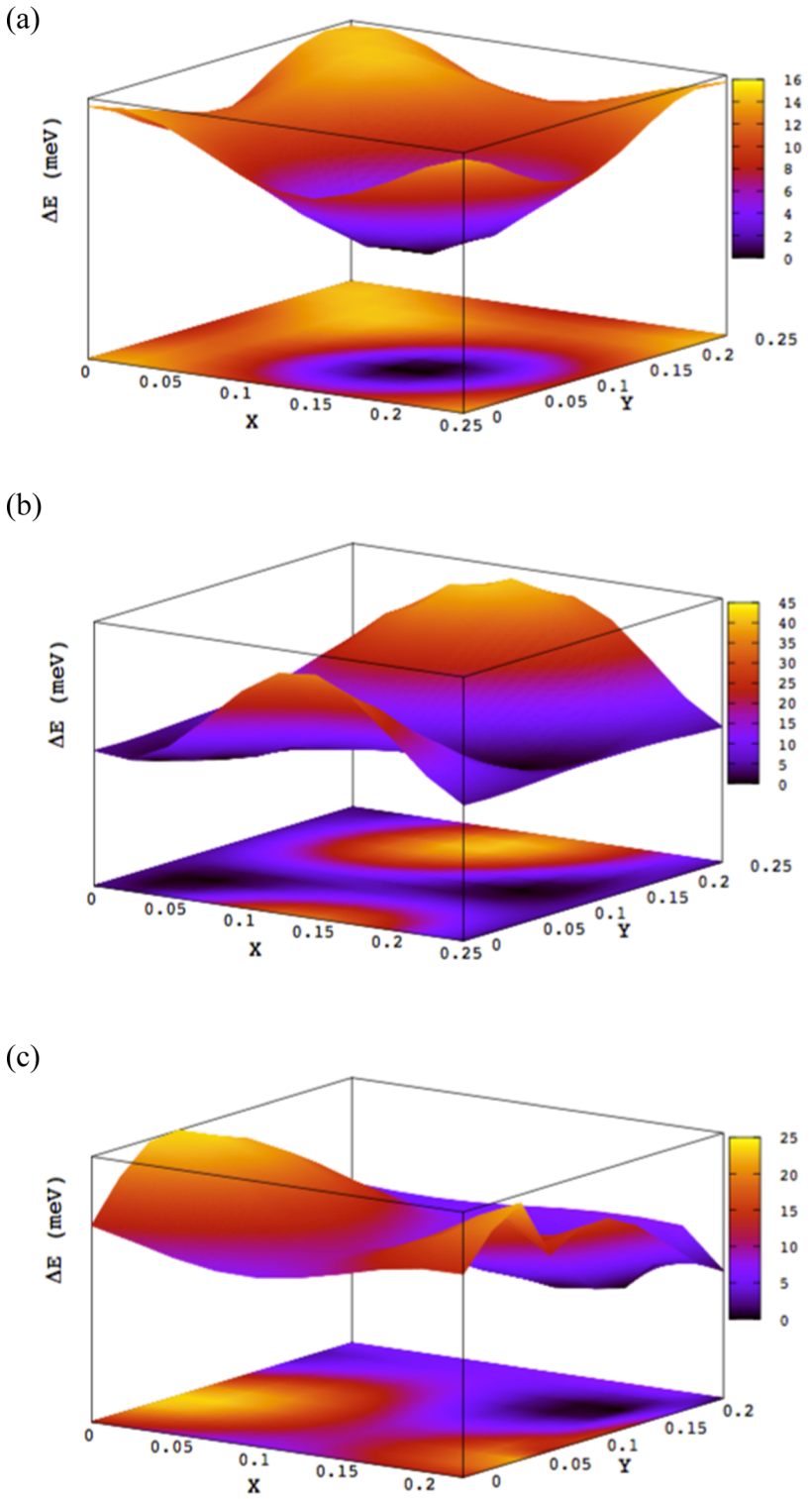

Figure 3. Binding potentials (3D local PES) and diffusion possibility of the selected VOCs on graphene: (a) ethanol on graphene, (b) benzene on graphene, and (c) toluene on graphene. The *X* and *Y* axes are fractional coordinates. The origin of the *X* and *Y* axes is the initial position of the COM of the VOC molecule. The vertical axis (ΔE) is the energy value that is shifted so that the most stable position corresponds to zero. In each figure, the upper color surface is a 3D image of PES, while the lower is the projected PES on the surface of a unit cell of graphene.

determined. The detailed calculation procedure can be summarized into two stages. First, one VOC molecule is horizontally scanned on the surface of a periodic part (one-unit cell of graphene) of the desired supercell to determine the stable position of the adsorbate on the surface of pristine graphene. Then, we scan along the vertical direction to determine the adsorption energy profile. The adsorption energies are calculated taking into account the contribution from the nonlocal van der Waals (vdW) exchange−correlation functionals by employing the revPBE-vdW, optPBE-vdW, and vdW-DF2 functionals. These functionals were shown to predict better results in the adsorption distances and energies

https://doi.org/10.1021/acsomega.3c06159
ACS Omega 2024, 9, 2302−2313

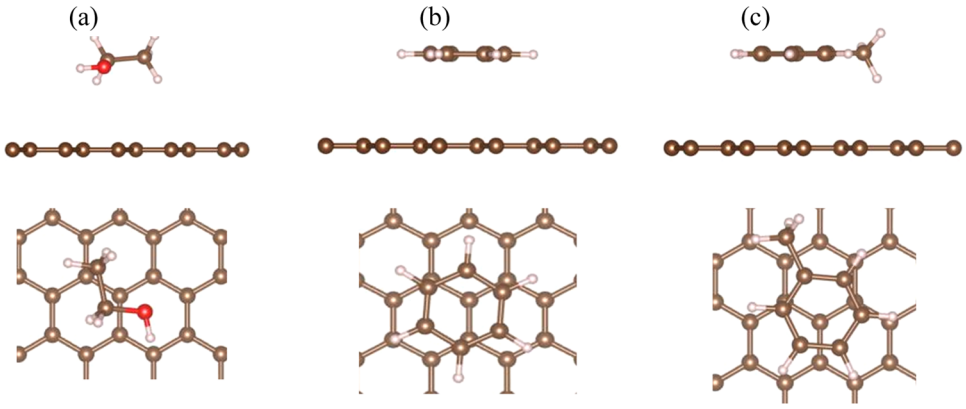

Figure 4. Side and top views (upper to lower) of the optimized structures of ethanol, benzene, and toluene on the pristine graphene with the VOC molecules oriented parallel to the graphene surface: (a) ethanol on graphene, (b) benzene on graphene, and (c) toluene on graphene.

of gas molecules on 2D material surfaces, including weak interactions. The revPBE-vdW[35] refers to the original vdW-DF proposed by Dion et al.[36] The optPBE-vdW functional is where the exchange functional was optimized for the correlation part,[37] and the vdW-DF2 is a second version of vdW-DF, developed by the Langreth and Lundqvist groups.[38] The vdW-DF and vdW-DF2 functionals used in this study have been implemented by Klimes[39] in VASP. The electronic properties of the adsorption systems were analyzed based on the band structure and the density of states (DOS). Charge distribution and charge transfer between the VOCs and pristine graphene are analyzed using the Bader charge analysis method.[40,41]

3. RESULTS AND DISCUSSION

3.1. Geometrical Structures of the Isolated VOCs and Graphene. The optimized geometrical structures of the isolated ethanol, benzene, and toluene molecules are represented in Figure 1. Ethanol's chemical formula is C_2H_6O. This chemical formula can also be written as CH_3CH_2OH. It is made of nine atoms, including two carbon (C) atoms, six hydrogen (H) atoms, and one oxygen (O) atom. There are two types of bonds in ethanol. The C−H bonds are nonpolar covalent since these atoms are of similar electronegativity. The C−O and O−H bonds are polar covalent since O is significantly more electronegative than either C or H. The geometry shows that there is a separation of the center of slight positive and slight negative in the molecule, which makes the ethanol molecule polar. Benzene is an organic chemical compound with the molecular formula C_6H_6, represented diagrammatically as a ring. The benzene molecule is composed of six carbon atoms joined in a planar ring, with one hydrogen atom attached to each. All six carbon−carbon bonds in benzene are of the same length, about 1.403 Å. The electrons of C═C bonding are distributed equally among each of the six carbon atoms. Toluene's chemical formula is $C_6H_5CH_3$, known as methylbenzene. The methyl C−H bonds are, on average, 0.011 Å longer than the ring C−H bonds. While the average ring C−C and C−H distances are nearly identical with those of benzene, the ring exhibits marked asymmetry, including an unexpected coupling between the ring C−C distances and the angle of methyl rotation.

It is important for our present comparative study to start with the structural and electronic properties of pristine graphene. The calculated C−C bonds in the optimized structure are found to be 1.43 Å, which is slightly larger than the ideal graphene's C−C bond length (1.42 Å). The electronic band structure of pristine graphene along the principal directions of the hexagonal Brillouin zone is plotted in Figure 2. It clearly shows that the band structure of pristine graphene has a zero-gap at the *K*-point, indicating semiconducting behavior. The pristine graphene work function is calculated to be 4.562 eV, which is in excellent agreement with theoretical and experimental values in the literature.[42,43] Using this optimized structure of graphene, we then investigated the adsorption properties of ethanol, benzene, and toluene onto pristine graphene.

3.2. Potential Energy Surface and Adsorption Configurations. The stable positions of adsorbates can be deduced from the minima on the potential energy surface (PES), as shown in Figure 3. The color gradient represents the relative energy, with dark purple and black regions indicating low energy and corresponding to favorable adsorption sites, while bright and yellow regions indicating high energy represent unfavorable sites. Possible diffusion pathways are shown in Figure 3, with *X* and *Y* being fractional coordinates based on the lattice vectors of the *XY*-plane of the supercell in the simulation model. The minimum energy diffusion pathways between the most stable sites are included. For the case of ethanol on graphene and toluene on graphene in Figure 3a,c, the PES showed a localized adsorption area, while the adsorption area of benzene on graphene in Figure 3b is delocalized. The dark regions indicate the diffusion paths, while the bright regions indicate that the VOC molecules are less preferable to be adsorbed on the graphene surface, as shown in Figure 3a−c. From Figure 3b, the diffusion channels of benzene on graphene are determined. The obtained results shown in three-dimensional (3D) local PES clarify the roles of the adsorption sites and the diffusion pathway of benzene. For ethanol, the estimated diffusion barrier is rather low, at approximately 16 meV. In the case of benzene and toluene, the diffusion barriers are estimated as 45 and 25 meV, respectively.

The difference in diffusion barriers could affect the sensor response. In order to detect the change in the electric current signal, the change in the resistance of the sensor should be sufficient. The resistance of the sensor gradually changes as more and more VOCs are adsorbed on the surface of graphene.

After the relaxation process of the minimum energy configurations of the considered VOC molecules on the

https://doi.org/10.1021/acsomega.3c06159
ACS Omega 2024, 9, 2302−2313

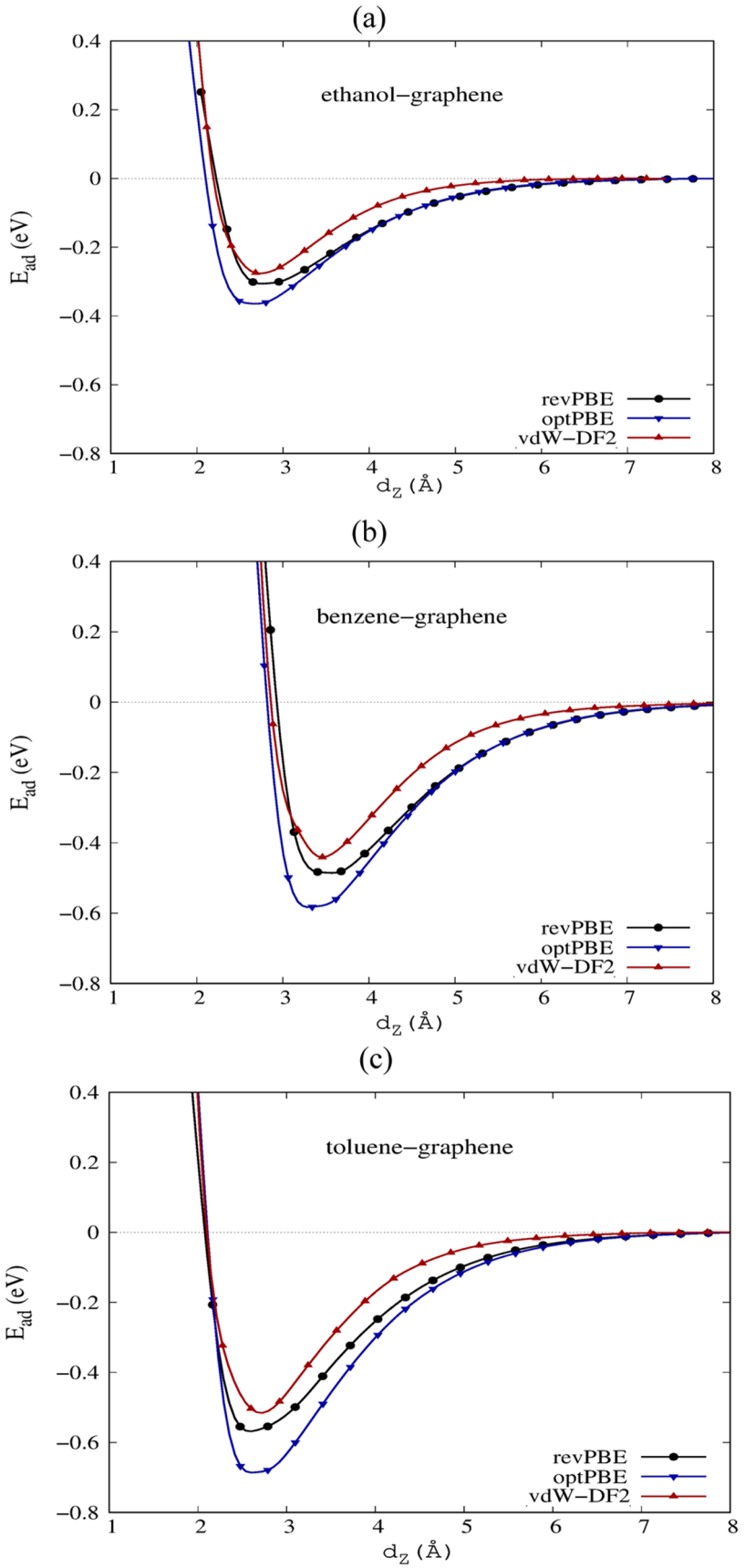

Figure 5. Adsorption energy profiles of ethanol, benzene, and toluene on graphene vs different van der Waals interactions. The horizontal axis d_z represents the distance from the graphene surface to the closest atom of the molecule; the vertical axis corresponds to the adsorption energy at various d_z: (a) ethanol on graphene, (b) benzene on graphene, and (c) toluene on graphene.

https://doi.org/10.1021/acsomega.3c06159
ACS Omega 2024, 9, 2302−2313

Table 1. Characteristics of Ethanol Adsorption on Graphene

dispersion/characteristics	revPBE-vdW	optPBE-vdW	vdW-DF2	exp.[18,19]
distance d_z (Å)	2.80	2.60	2.45	na
distance d_{z_c} (Å)	3.65	3.44	3.25	na
response length (Å)	8.44	8.09	6.82	na
recovery time τ (s)	1.38×10^{-7}	1.25×10^{-6}	4.32×10^{-8}	na
adsorption energy (meV)	306	363	276	350 ± 30

Table 2. Characteristics of Benzene Adsorption on Graphene

dispersion/characteristics	revPBE-vdW	optPBE-vdW	vdW-DF2	exp.
distance d_z (Å)	3.45	3.35	3.17	na
distance d_{z_c} (Å)	3.47	3.36	3.19	3.60[44] 3.17[45]
response length (Å)	9.54	9.24	9.19	na
recovery time τ (s)	1.34×10^{-4}	5.94×10^{-3}	2.1×10^{-5}	na
adsorption energy (meV)	484	582	436	516 ± 13[21]

Table 3. Characteristics of Toluene Adsorption on Graphene

dispersion/characteristics	revPBE-vdW	optPBE-vdW	vdW-DF2	exp.[19]
distance dz (Å)	2.65	2.65	2.35	na
distance d_{z_c} (Å)	3.60	3.42	3.20	na
response length (Å)	8.23	8.16	7.74	na
recovery time τ (s)	3.2×10^{-3}	0.332	4.6×10^{-4}	na
adsorption energy (meV)	566	686	516	585 ± 13

graphene surface obtained from the scanning method, all of these VOCs are found to orient parallel to the graphene surface at the range of 3.47−3.65 Å (from the COM of the VOCs) above the graphene surface, as shown in Figure 4. These distances are consistent with the experimental values, which are estimated from binding energy curves performed by Chakarova-Käck et al.[44] and Zhang et al.[45]

The optimized structures of the adsorption systems show that adsorption does not result in changes to the chemical bonding structures of both VOCs and graphene. The orientation of the functional group −OH of the adsorbed ethanol molecule to the graphene surface is the most preferable. In the cases of benzene and toluene, the lowest energy configurations are with the aromatic ring parallel to the graphene surface and the center of the aromatic ring of the molecule on top of a graphene carbon atom.

3.3. Adsorption Energy Profiles. To investigate and assess the interaction between the substrate and adsorbate, we explore the adsorption energy profile of ethanol, benzene, and toluene on graphene. Adsorption energy values of ethanol, benzene, and toluene on graphene with different van de Waals interactions are shown in Figure 5 and Tables 1, 2, and 3. The horizontal axis represents the distance (Å) from the COM of the VOCs to the graphene surface. The adsorption energy is defined as

$$E_{\text{adsorption}} = E_{\text{complex}} - E_{\text{saturation}} \quad (1)$$

in which E_{complex} represents the total energy of the adsorbed system (the VOCs and graphene), and $E_{\text{saturation}}$ stands for the total energy of the configuration of the complex system in which the VOC molecules and graphene are isolated from each other. This formula is equivalent to

$$E_{\text{adsorption}} = E_{\text{complex}} - E_{\text{VOC}} - E_{\text{graphene}} \quad (2)$$

where E_{VOC} and E_{graphene} refer to the total relaxed energy of the isolated VOC molecules and graphene, respectively.

As we can see in Figure 5 and Tables 1−3, the adsorption energy ranges in the sequence of vdW-DF2 < revPBE-vdW < optPBE-vdW. The experimental data of adsorption energies are also listed in these tables for comparison. For all cases of ethanol, benzene, and toluene on pristine graphene, the adsorption energies calculated by revPBE-vdW are in good agreement with the available experimental data,[19,21,44] indicating that the revPBE functional can cover physical phenomena behind adsorption of these VOCs on graphene sufficiently well. On the other hand, the results obtained using vdW-DF2 differ significantly. According to the calculated values of the adsorption energies, these selected VOC molecules are physically adsorbed on the graphene surface. Therefore, we predict an inconsiderable change in the geometric and thermodynamic properties of the gas molecules arising from the interaction with graphene.

Tables 1−3 represent the optimal adsorption distances from the closest atom of the VOC molecules to the graphene d_z and from the COM of the molecule to the graphene surface d_{z_c} at full relaxation for the adsorption of ethanol, benzene, and toluene, respectively. The shortest distance d_z is around 2.35−2.65 Å for these selected VOCs (revPBE-vdW dispersion). These distance values overcome the chemical interaction limit between the H and the O atoms, indicating again the physisorption of VOC gases onto graphene.

Here, we refer to the response length as the threshold distance at distances further than which there is no interaction between VOCs and the graphene surface. At this distance, the adsorption energy equals to zero, as shown in Figure 5. Response length can be expected to play a role in determining the response rate of the sensor. The response lengths for the adsorption of three VOC gases on graphene are quite small, less than 10, as shown in Tables 1−3. As the VOC molecule

https://doi.org/10.1021/acsomega.3c06159
ACS Omega 2024, 9, 2302−2313

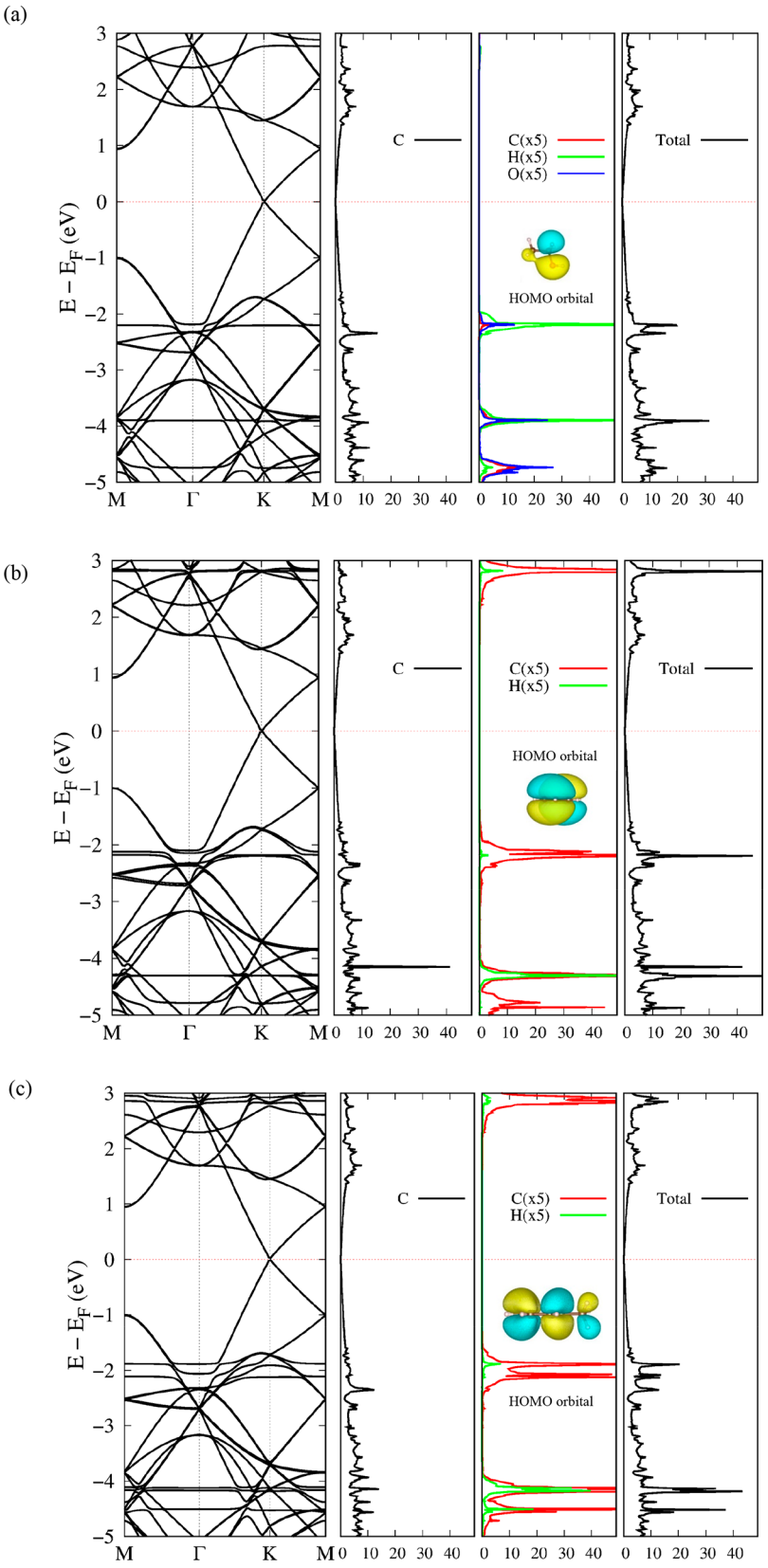

Figure 6. Band structures along the *M*−Γ−*K*−*M* path of the irreducible Brillouin zone (left) and DOS of individual VOCs on graphene calculated by the revPBE-vdW functional (three right panels): (a) ethanol on graphene, (b) benzene on graphene, and (c) toluene on graphene. The second panel from the left illustrates DOS of graphene, the third is of adsorbed molecule, and the fourth is the total DOS of the adsorbed system. The inset is the charge density of the molecule HOMO in adsorption. The dashed lines represent the Fermi level. DOS is in units of state/eV.

https://doi.org/10.1021/acsomega.3c06159
ACS Omega 2024, 9, 2302−2313

Table 4. Band Gap Energy, Charge Transfers from the Graphene Surface to the VOC Molecules, and the Work Function Obtained by revPBE-vdW

	ethanol on graphene	benzene on graphene	toluene on graphene
band gap (meV)	6	5	12
charge transfer (e)	0.064	0.043	0.061
work function (eV)	4.343	4.394	4.398

descends onto the surface of graphene, a shorter response length might allow a faster change in the electronic properties of graphene.

The recovery time τ is the time required for gas molecules to fully dislodge from the adsorbent, which is calculated by the expression

$$\tau = \upsilon^{-1} \exp\left(-\frac{E_a}{k_B T}\right) \quad (3)$$

in which υ, k_B, and T are the attempt frequency, Boltzmann constant, and temperature, respectively. The theoretical values of the recovery times at room temperature (300 K) for the interaction of three VOCs on graphene are presented in Tables 1−3. These values are all less than 0.33 s, depending on the functionals used. The short recovery time implies the almost instantaneous desorption of graphene to the VOC gases. In such a rapid response time, it is difficult to significantly alter the vibrational partition functions as well as the translational and rotational degrees of freedom of the gas molecules due to their adsorption on graphene.

3.4. Density of States and Electronic Band Structure.

To investigate the nature of the selected VOCs' adsorption on graphene, we calculated the band dispersion along high symmetry k-points and DOS of the VOCs adsorbed on graphene. Band structures and the DOS of the considered VOCs on graphene by the revPBE-vdW functional are shown in Figure 6. After the adsorption of the selected VOCs on graphene, the electronic band structure of graphene along the $M-\Gamma-K-M$ path of irreducible Brillouin zone displays a gap opening at around K-point, as indicated in ref 46 The band gap energies for the adsorption of ethanol, benzene, and toluene on graphene are 6, 5, and 12 meV, respectively (see Table 4). The large band gap in the case of toluene adsorption might be related to the largest adsorption energy compared to ethanol and benzene. Opening a band gap might lead to the decrease of electrical conductivity, which implies the possibility of detecting VOCs by monitoring the conductance of graphene upon exposure to a breath containing VOCs. Gap opening also exhibits a lower carrier concentration after gas adsorption, driving the resistance upward. Toluene opens the largest band gap, which indicates the strongest effect on the sensor signal, in accordance with the largest adsorption energy. Among the selected VOCs, toluene tends to adsorb on the graphene better than ethanol and benzene. Additionally, by comparing the DOS image of adsorption systems shown in Figure 6 to that of the isolated VOC molecules in Figure S1 in the Supporting Information, we found that the highest occupied molecular orbitals (HOMO) of these considered VOCs are shifted downward from the Fermi level. Moreover, the HOMO states of the VOCs become delocalized due to the interaction with the p orbitals of C graphene. These results suggest the charge acceptance tendency of the VOC molecules from graphene. These VOC molecules are physically adsorbed on the graphene surface with a rather small adsorption energy (300−550 meV), and the adsorbed VOC molecules do not strongly alter the electronic structure of graphene in general, as shown by the band structure and total DOS of graphene before and after adsorption in Figures 2b and 6, respectively. However, changes occur in the projected DOS of C atoms of graphene, which interact with the VOC molecules, as shown in Figure 7. It shows the different orbital contributions to the DOS of C graphene before and after the VOCs adsorption, especially the p_y orbital and more p_x orbital contribution, which appeared on the DOS of C graphene near the VOC molecules. We found that the adsorption of these VOC molecules causes hybridizations between the molecular levels and the graphene valence bands. The interaction of the VOCs with π and π^* states of the C atoms in graphene breaks the symmetry of graphene, and a band gap occurs at the Fermi level. The interactions and hybridizations transform the zero-gap semiconductor graphene into the milli-gap graphene.

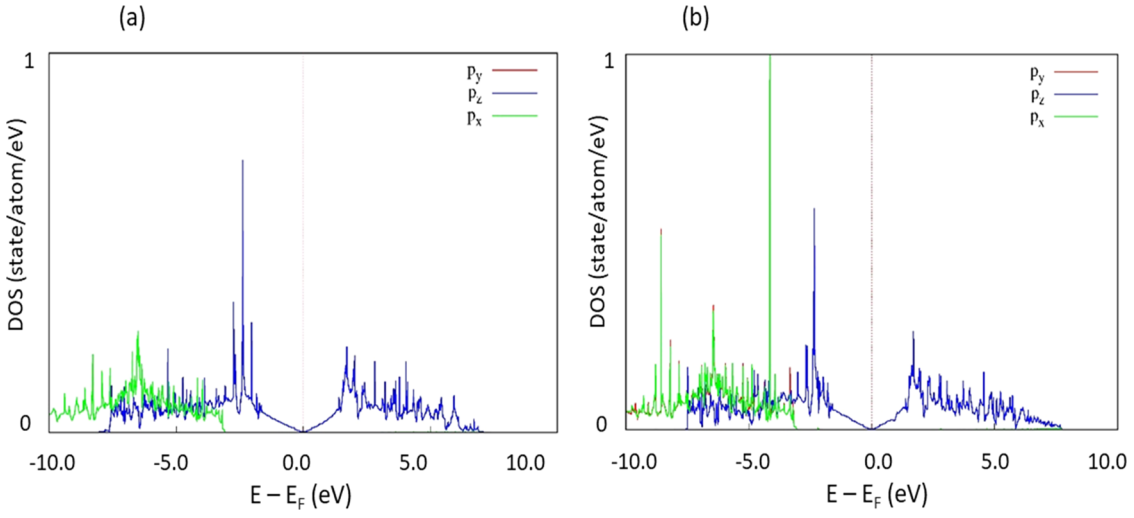

Figure 7. Partial DOS of C atom in graphene before (a) and after (b) the VOC adsorption for the atom that is nearest to the benzene molecule in the adsorption system.

https://doi.org/10.1021/acsomega.3c06159
ACS Omega 2024, 9, 2302−2313

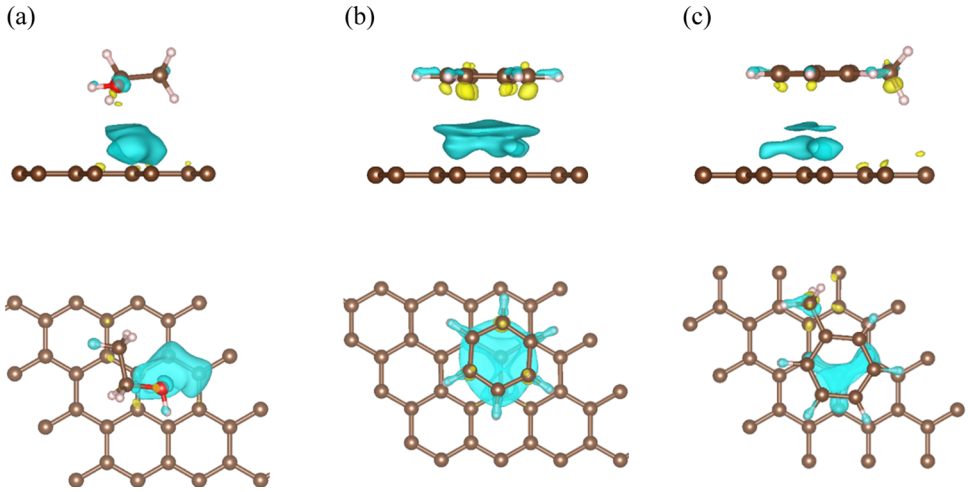

Figure 8. Side and top views (upper to lower) of charge density difference induced by the adsorption of ethanol (a), benzene (b), and toluene (c) on graphene. The isosurface value is ±0.03 e Å^{-2}. The blue region represents the electron donor, and the yellow region represents the electron acceptor, respectively.

3.5. Work Function and Charge Transfer. The work function (WF) is defined as the energy necessary to remove an electron originally at the Fermi level (EF) inside the surface and place it at rest at a point in free space just outside the surface, i.e., bringing an electron from the surface Fermi level to the vacuum.[47] Electrons are naturally bound to the solid. At the surface of the material, they are prevented from escaping (to the vacuum) by an energy barrier that culminates at the vacuum level (E_{VAC}). The work function WF = $E_{VAC} - E_F$ represents the energy barrier to free space that prevents an electron at the Fermi level from escaping from the solid. The energy position of E_{VAC} is accurately measured by detecting the lowest energy electrons that escape from the solid under photoexcitation. As mentioned above, the WF of pristine graphene in our calculation is 4.562 eV. When the considered VOC adsorption occurs, the WF of the complex system is found to be 4.343, 4.394, and 4.398 eV for ethanol, benzene, and toluene on graphene, respectively, as summarized in Table 4. The WF values of the complex systems are reduced as compared to the pristine graphene WF. The adsorption energy and work function for these adsorption systems follow a roughly proportional relationship. This is very useful for predicting the stability of the surface.

Next, a Bader analysis is performed to predict the charge-transfer value. The charge density difference provides information about the charge accumulation and charge depletion regions. The charge density difference of a system AB is determined by $\Delta\rho = \rho_{AB} - \rho_A - \rho_B$, where ρ_i stands for the charge density of the corresponding system i. In some cases, it intuitively indicates where bonds are made or destroyed if chemical adsorption occurs. Although different methods, in addition to Bader analysis, may give rise to different values in determining the electronic charge transfer, the trend and order of magnitude should be the same. By comparison of the charge before and after adsorption of the VOC molecules, the magnitude and direction of charge transfer can be inferred. The results of charge-transfer analysis of the selected VOCs on graphene are shown in Table 4. The charge density difference induced by the adsorption of ethanol, benzene, and toluene on graphene is plotted in Figure 8.

All considered VOCs act as electron acceptors from graphene. It is noticed that there are differences in the number of electrons transferred from graphene to the VOCs and in the distance between the VOCs and graphene. They are correlated because a smaller distance between the VOC molecules and graphene leads to a larger orbital overlap and, consequently, more orbital mixing (i.e., larger charge transfers). Comparing the adsorption of toxic gases (NH_3, NO, NO_2, CO, CO_2···) on the graphene surface,[48] the charge transferred from graphene to the VOCs is larger than those from the graphene surface to toxic gases (0.012−0.028e). The charge transferred between the considered VOCs and graphene is found not to strongly depend on the distance between the adsorbate and the graphene surface. This reflects the fact that electron transfer in VOC-graphene systems is quite complex. The electron can move from the substrate to one of the ions in the adsorbed molecule, while a part of charge transfers back to the graphene surface at other positions might occur, resulting in the nonlinear relationship between the number of transferred electrons and the distance between graphene and VOC molecules.

Interestingly, ethanol behaves as a weakly adsorbed molecule and shows a small adsorption energy, unexpectedly opening a similar band gap (5−6 meV) as the case of benzene. The charge analysis revealed that there is no significant difference in the number of electrons transferred from the graphene surface to the VOC molecules of ethanol (0.064e), benzene (0.043e), and toluene (0.061e). Apparently, there is no linear relationship between the magnitude of the charge transfer and the adsorption energy or the band gap opening. It could be due to the band gap opening of graphene being in relation to the charge transfer between not only the HOMO/lowest unoccupied molecular orbital (HOMO/LUMO) levels but also to the deeper levels in the valence bands of adsorption systems.

4. CONCLUSIONS

This study systematically investigated the adsorption mechanism of ethanol, benzene, and toluene on graphene using nonlocal van der Waals density functional theory. The most energetically favorable configurations of adsorbed systems, adsorption energy profiles, charge transfer, and work functions were determined. The calculated adsorption energies using revPBE-vdW are in good agreement with the experimental

https://doi.org/10.1021/acsomega.3c06159
ACS Omega 2024, 9, 2302−2313

data. The lowest adsorption energy is found for ethanol, and the highest is found for toluene. The revPBE-vdW functional effectively captures the physical phenomena behind the adsorption of these VOCs on graphene. Bader charge analysis indicates that 0.064*e*, 0.043*e*, and 0.061*e* of charge are transferred from graphene to ethanol, benzene, and toluene, respectively, which are consistent with the images of charge density difference. Therefore, VOC adsorption can cause a reduction in the graphene conductivity. The uplifting of the highest occupied molecular orbitals of these VOCs to the Fermi level is observed by analyzing the electronic structure of adsorption systems. We predict that the interaction of the VOCs with π and π^* states of the C atoms in graphene breaks the symmetry of graphene, leading to the opening of a band gap at the Fermi level of about 5−12 meV.

The results indicate that graphene is sensitive to these considered VOCs and could have possible applications in VOC sensors for detecting cancer through exhaled breath. This work opens the way for further studies of graphene and other 2D materials toward their fascinating sensing properties and their application in high-performance chemical and biochemical sensors.

■ ASSOCIATED CONTENT

Supporting Information

The Supporting Information is available free of charge at https://pubs.acs.org/doi/10.1021/acsomega.3c06159.

Projected density of states of individual elements of isolated VOCs are displayed and analyzed (PDF)

■ AUTHOR INFORMATION

Corresponding Authors

Viet Bac T. Phung − *Institute of Sustainability Science, VNU Vietnam Japan University, Hanoi 1000000, Vietnam; Center for Environmental Intelligence and College of Engineering & Computer Science, VinUniversity, Hanoi 100000, Vietnam;* orcid.org/0000-0001-7717-2538; Email: bac.ptv@vinuni.edu.vn

Van An Dinh − *Department of Precision Engineering, Graduate School of Engineering, Osaka University, Suita, Osaka 565-0871, Japan;* orcid.org/0000-0002-7290-7969; Email: divan@prec.eng.osaka-u.ac.jp

Authors

Thi Nhan Tran − *Faculty of Fundamental Sciences, Hanoi University of Industry, Hanoi 100000, Vietnam*

Quang Huy Tran − *Faculty of Physics, Hanoi Pedagogical University 2, Phuc Yen, Vinh Phuc 280000, Vietnam*

Thi Theu Luong − *Hoa Binh University, Hanoi 100000, Vietnam*

Complete contact information is available at: https://pubs.acs.org/10.1021/acsomega.3c06159

Author Contributions

All authors have approved the final version of the manuscript.

Notes

The authors declare no competing financial interest.

■ ACKNOWLEDGMENTS

The authors acknowledge the facility support from the JICA Technical Cooperation project at VNU Vietnam Japan University.

■ REFERENCES

(1) Schnabel, R.; Fijten, R.; Smolinska, A.; Dallinga, J.; Boumans, M.-L.; Stobberingh, E.; Boots, A.; Roekaerts, P.; Bergmans, D.; van Schooten, F. J. Analysis of Volatile Organic Compounds in Exhaled Breath to Diagnose Ventilator-Associated Pneumonia. *Sci. Rep.* **2015**, *5*, No. 17179.

(2) Ego, A.; Preiser, J.-C.; Vincent, J.-L. Impact of Diagnostic Criteria on the Incidence of Ventilator-Associated Pneumonia. *Chest* **2015**, *147* (2), 347−355.

(3) Boots, A. W.; van Berkel, J. J. B. N.; Dallinga, J. W.; Smolinska, A.; Wouters, E. F.; van Schooten, F. J. The Versatile Use of Exhaled Volatile Organic Compounds in Human Health and Disease. *J. Breath Res.* **2012**, *6* (2), No. 027108.

(4) Miekisch, W.; Schubert, J. K.; Noeldge-Schomburg, G. F. E. Diagnostic Potential of Breath Analysis—Focus on Volatile Organic Compounds. *Clin. Chim. Acta* **2004**, *347* (1−2), 25−39.

(5) Barker, M.; Hengst, M.; Schmid, J.; Buers, H.-J.; Mittermaier, B.; Klemp, D.; Koppmann, R. Volatile Organic Compounds in the Exhaled Breath of Young Patients with Cystic Fibrosis. *Eur. Respir. J.* **2006**, *27*, 929−936.

(6) Hakim, M.; Broza, Y. Y.; Barash, O.; Peled, N.; Phillips, M.; Amann, A.; Haick, H. Volatile Organic Compounds of Lung Cancer and Possible Biochemical Pathways. *Chem. Rev.* **2012**, *112* (11), 5949−5966.

(7) Gaspar, E. M.; Lucena, A. F.; da Costa, J. D.; das Neves, H. C. Organic Metabolites in Exhaled Human Breath-A Multivariate Approach for Identification of Biomarkers in Lung Disorders. *J. Chromatogr. A* **2009**, *1216* (14), 2749−2756.

(8) Dragonieri, S.; Annema, J. T.; Schot, R.; van der Schee, M. P. C.; Spanevello, A.; Carratú, P.; Resta, O.; Rabe, K. F.; Sterk, P. J. An Electronic Nose in the Discrimination of Patients with Non-Small Cell Lung Cancer and COPD. *Lung Cancer* **2009**, *64*, 166−170.

(9) Queralto, N.; Berliner, A. N.; Goldsmith, B.; Martino, R.; Rhodes, P.; Lim, S. H. Detecting Cancer by Breath Volatile Organic Compound Analysis : A Review of Array-Based Sensors. *J. Breath Res.* **2014**, *8*, 027112−027124.

(10) Konvalina, G.; Haick, H. Sensors for Breath Testing : From Nanomaterials to Comprehensive Disease Detection. *Acc. Chem. Res.* **2014**, *47* (1), 66−76.

(11) Algorithm, V. M. Diagnosis by Volatile Organic Compounds in Exhaled Breath from Lung Cancer Patients Using Support. *Sensors* **2017**, *17*, No. 287.

(12) Broza, Y. Y.; Haick, H. Nanomaterial-Based Sensors for Detection of Disease by Volatile Organic Compounds. *Nanomedicine* **2013**, *8* (5), 785−806.

(13) Jalal, A. H.; Alam, F.; Roychoudhury, S.; Umasankar, Y.; Pala, N.; Bhansali, S. Prospects and Challenges of Volatile Organic Compound Sensors in Human Healthcare. *ACS Sens.* **2018**, *3* (7), 1246−1263.

(14) Wang, Y.; Hu, Y.; Wang, D.; Yu, K.; Wang, L.; Zou, Y.; Zhao, C.; Zhang, X.; Wang, P.; Ying, K. The Analysis of Volatile Organic Compounds Biomarkers for Lung Cancer in Exhaled Breath, Tissues and Cell Lines. *Cancer Biomarkers* **2012**, *11* (4), 129−137.

(15) Saalberg, Y.; Wolff, M. VOC Breath Biomarkers in Lung Cancer. *Clin. Chim. Acta* **2016**, *459*, 5−9.

(16) Hohenberg, P.; Kohn, W. Inhomogeneous Electron Gas. *Phys. Rev.* **1964**, *136* (3B), B864−B871.

(17) Kohn, W.; Sham, L. J. Self-Consistent Equations Including Exchange and Correlation Effects. *Phys. Rev.* **1965**, *140* (4A), A1133−A1138.

(18) Karlický, F.; Otyepková, E.; Banáš, P.; Lazar, P.; Kocman, M.; Otyepka, M. Interplay between Ethanol Adsorption to High-Energy Sites and Clustering on Graphene and Graphite Alters the Measured Isosteric Adsorption Enthalpies. *J. Phys. Chem. C* **2015**, *119* (35), 20535−20543.

(19) Lazar, P.; Karlický, F.; Jurecka, P.; Kocman, M.; Otyepková, E.; Šafářová, K.; Otyepka, M. Adsorption of Small Organic Molecules on Graphene. *J. Am. Chem. Soc.* **2013**, *135* (16), 6372−6377.

(20) Leenaerts, O.; Partoens, B.; Peeters, F. M. Graphene: A Perfect Nanoballoon. *Appl. Phys. Lett.* **2008**, *93* (19), 91−94.
(21) Otyepková, E.; Lazar, P.; Čépe, K.; Tomanec, O.; Otyepka, M. Organic Adsorbates Have Higher Affinities to Fluorographene than to Graphene. *Appl. Mater. Today* **2016**, *5*, 142−149.
(22) Burke, K. Perspective on Density Functional Theory. *J. Chem. Phys.* **2012**, *136* (15), No. 150901.
(23) Cohen, A. J.; Mori-Sanchez, P.; Yang, W. T. J. Challenges for Density Functional Theory. *Chem. Rev.* **2012**, *112*, 289−320.
(24) Wu, C.; Wang, L.; Xiao, Z.; Li, G.; Wang, L. Effects of van der Waals Interactions on the Dehydrogenation of n-butane on a Ni(111) Surface. *Chem. Phys. Lett.* **2020**, *746*, No. 137299.
(25) Karlický, F.; Otyepková, E.; Lo, R.; Pitoňák, M.; Jurečka, P.; Pykal, M.; Hobza, P.; Otyepka, M. Adsorption of Organic Molecules to Van der Waals Materials: Comparison of Fluorographene and Fluorographite with Graphene and Graphite. *J. Chem. Theory Comput.* **2017**, *13*, 1328−1340.
(26) Deng, X.; Gao, T.; Dai, J. Temperature dependence of adsorption and desorption dynamics of NO_2 molecule on boron-doped graphene. *Phys. E* **2022**, *137*, No. 115083.
(27) Göltl, F.; Hafner, J. Modelling the adsorption of short alkanes in protonated chabazite: The impact of dispersion forces and temperature. *Microporous Mesoporous Mater.* **2013**, *166*, 176−184.
(28) Menezes, I. R. S.; Sakai, T.; Hattori, Y.; Kaneko, K. Effect of preheating temperature on adsorption of N_2 and Ar on graphene oxide. *Chem. Phys. Lett.* **2022**, *807*, No. 140091.
(29) Phung, T. V. B.; Ogawa, H.; Dinh, V. A.; Nguyen, H. O.; Shibutani, Y.; Asano, K.; Nakamura, Y.; Akiba, E. Effects of substitutional Mo and Cr on site occupation and diffusion of hydrogen in the β-phase vanadium hydride by first principles calculations. *Theor. Chem. Acc.* **2019**, *138*, No. 16.
(30) Kresse, G.; Furthmüller, J. Efficient Iterative Schemes for Ab Initio Total Energy Calculations Using a Plane-wave Basis Set. *Phys. Rev. B* **1996**, *54*, 11169−11186.
(31) Ta, L. T.; Hamada, I.; Morikawa, Y.; Dinh, V. A. Adsorption of Toxic Gases on Borophene: Surface Deformation Links to Chemisorptions. *RSC Adv.* **2021**, *11* (30), 18279−18287.
(32) Phung, V. B. T.; Pham, T. L.; Dinh, V. A. Adsorption of 2-Butanone on Pristine Graphene: A First-Principles Study. *VNU J. Sci.: Math.-Phys.* **2020**, *36* (1), 71−79.
(33) Pham, T. L.; Ta, T. L.; Vo, V. O.; Dinh, V. A. DFT Study on Adsorption of Acetone and Toluene on Silicene. *VNU J. Sci.: Math.-Phys.* **2020**, *36* (1), 95−102.
(34) Ta, T. L.; Pham, T. L.; Dinh, V. A. Toxic Gases on B12 Borophene: The Selective Adsorption. *VNU J. Sci.: Math.-Phys.* **2020**, *36* (2), 66−73.
(35) Román-Pérez, G.; Soler, J. M. Efficient implementation of a van der Waals density functional: Application to double-wall carbon nanotubes. *Phys. Rev. Lett.* **1999**, *103*, No. 096102.
(36) Dion, M.; Rydberg, H.; Schröder, E.; Langreth, D. C.; Lundqvist, B. I. Van Der Waals Density Functional for General Geometries. *Phys. Rev. Lett.* **2004**, *92* (24), 22−25.
(37) Klimeš, J.; Bowler, D. R.; Michaelides, A. Chemical Accuracy for the van Der Waals Density Functional. *J. Phys.: Condens. Matter* **2010**, *22* (2), 22201−22205.
(38) Lee, K.; Murray, É. D.; Kong, L.; Lundqvist, B. I.; Langreth, D. C. Higher-Accuracy van Der Waals Density Functional. *Phys. Rev. B* **2010**, *82*, No. 081101(R).
(39) Klimeš, J.; Bowler, D. R.; Michaelides, A. Van Der Waals Density Functionals Applied to Solids. *Phys. Rev. B* **2011**, *83* (19), No. 195131.
(40) Henkelman, G.; Uberuaga, B. P.; Jónsson, H. Climbing Image Nudged Elastic Band Method for Finding Saddle Points and Minimum Energy Paths. *J. Chem. Phys.* **2000**, *113* (22), 9901−9904.
(41) Henkelman, G.; Arnaldsson, A.; Jónsson, H. A Fast and Robust Algorithm for Bader Decomposition of Charge Density. *Comput. Mater. Sci.* **2006**, *36* (3), 354−360.
(42) Filleter, T.; Emtsev, K. V.; Seyller, T.; Bennewitz, R. Local Work Function Measurements of Epitaxial Graphene. *Appl. Phys. Lett.* **2008**, *93*, No. 133117.
(43) Yu, Y.-J.; Zhao, Y.; Ryu, S.; Brus, L. E.; Kim, K. S.; Kim, P. Tuning the Graphene Work Function by Electric Field Effect. *Nano Lett.* **2009**, *9* (10), 3430−3434.
(44) Chakarova-Käck, S. D.; Schröder, E.; Lundqvist, B. I.; Langreth, D. C. Application of van Der Waals Density Functional to an Extended System: Adsorption of Benzene and Naphthalene on Graphite. *Phys. Rev. Lett.* **2006**, *96* (14), No. 146107.
(45) Zhang, Y. H.; Zhou, K. G.; Xie, K. F.; Zeng, J.; Zhang, H. L.; Peng, Y. Tuning the Electronic Structure and Transport Properties of Graphene by Noncovalent Functionalization: Effects of Organic Donor, Acceptor and Metal Atoms. *Nanotechnology* **2010**, *21* (6), No. 065201.
(46) Chang, C.-H.; Fan, X.; Li, L.-J.; Kuo, J.-L. Band Gap Tuning of Graphene by Adsorption of Aromatic Molecules. *J. Phys. Chem. C* **2012**, *116*, 13788−13794.
(47) Kahn, A. Fermi Level, Work Function and Vacuum Level. *Mater. Horiz.* **2016**, *3* (1), 7−10.
(48) Leenaerts, O.; Partoens, B.; Peeters, F. M. Adsorption of H_2O, NH_3, CO, NO_2, and NO on Graphene: A First-Principles Study. *Phys. Rev. B* **2008**, *77* (12), 1254161−1254166.

https://doi.org/10.1021/acsomega.3c06159
ACS Omega 2024, 9, 2302−2313